

# Highly Luminescent Monodisperse CdSe and CdSe/ZnS Nanocrystals Synthesized in a Hexadecylamine–Trioctylphosphine Oxide–Trioctylphosphine Mixture

Dmitri V. Talapin,<sup>\*,†</sup> Andrey L. Rogach,<sup>†</sup> Andreas Kornowski, Markus Haase, and Horst Weller<sup>‡</sup>

*Institute of Physical Chemistry, University of Hamburg, Bundesstrasse 45, 20146 Hamburg, Germany*

Received January 30, 2001

## ABSTRACT

Highly monodisperse CdSe nanocrystals were prepared in a three-component hexadecylamine–trioctylphosphine oxide–trioctylphosphine (HDA–TOPO–TOP) mixture. This modification of the conventional organometallic synthesis of CdSe nanocrystals in TOPO–TOP provides much better control over growth dynamics, resulting in the absence of defocusing of the particle size distribution during growth. The room-temperature quantum efficiency of the band edge luminescence of CdSe nanocrystals can be improved to 40–60% by surface passivation with inorganic (ZnS) or organic (alkylamines) shells.

Chemically grown CdSe nanocrystals (also referred to as quantum dots) are probably the most extensively investigated object among semiconductor nanoparticles since the introduction of the concept of the “size quantization effect” in the earlier eighties.<sup>1,2</sup> This is caused to a large extent by the existence of a very successful preparation method for high-quality CdSe nanocrystals, i.e., arrested precipitation in high boiling mixtures of trioctylphosphine oxide (TOPO) and trioctylphosphine (TOP).<sup>3,4</sup> The term “high-quality quantum dots” has been recently defined as follows:<sup>5</sup> the achievement of desired particle sizes over the largest possible range, narrow size distributions, good crystallinity, desired surface properties, and in the case of luminescent materials, high quantum yield. CdSe nanocrystals prepared by the TOPO–TOP route and size-separated after synthesis meet all these requirements apart from the last—high luminescence quantum yield, which does not exceed 5–15% for as-prepared particles.<sup>6–8</sup> The luminescence quantum efficiency can be sufficiently improved by growing heteroepitaxially an inorganic shell of the wide-band gap semiconductor around the particles.<sup>6–9</sup> The conventional techniques used for the wide-band gap shell growth, however, allow us to prepare only very small amounts of core–shell nanoparticles. Another problem of the TOPO–TOP synthesis is the

irreproducibility of the growth dynamics and the shape of the CdSe nanocrystals conditioned by an uncertain composition of the coordinating solvent. Technical grade TOPO (90%, Strem or Aldrich), for instance, provides better conditions for the growth of CdSe nanocrystals than distilled TOPO.<sup>10</sup> Recent developments of the organometallic synthetic routes to II–VI semiconductor nanocrystals included an introduction of hexylphosphonic acid to the TOPO–TOP mixture<sup>10–12</sup> and use of hexadecylamine (HDA) as the capping agent for pure and doped ZnSe nanocrystals.<sup>13,14</sup>

Taking into account the growing demand on highly luminescent semiconductor nanocrystals for light-emitting devices<sup>15–17</sup> and tagging applications,<sup>18,19</sup> we tried to improve the conventional organometallic TOPO–TOP synthesis by introducing an additional coordinating component (HDA) to the TOPO–TOP mixture. In this mixture focusing of the size distribution is observed during particle growth so that no postpreparative size-selective precipitation is required. The surface of as-prepared CdSe nanocrystals can be passivated without isolating the nanocrystals from the crude solution either by growing an inorganic shell or by surface modification with alkylamines. Both methods lead to stable and reproducible luminescence quantum efficiencies (QE) of ~50% at room temperature. The high quality of these CdSe quantum dots has been confirmed by absorption and photoluminescence (PL) spectroscopy, powder X-ray diffraction (P-XRD) and high-resolution transmission electron microscopy (HRTEM).

\* Corresponding author. E-mail address: talapin@chemie.uni-hamburg.de. Fax: +49–40–42838-3452.

<sup>†</sup> On leave from Physico-Chemical Research Institute, Belarusian State University, 220050 Minsk, Belarus.

<sup>‡</sup> Homepage: <http://www.chemie.uni-hamburg.de/pc/AKs/Weller/>.

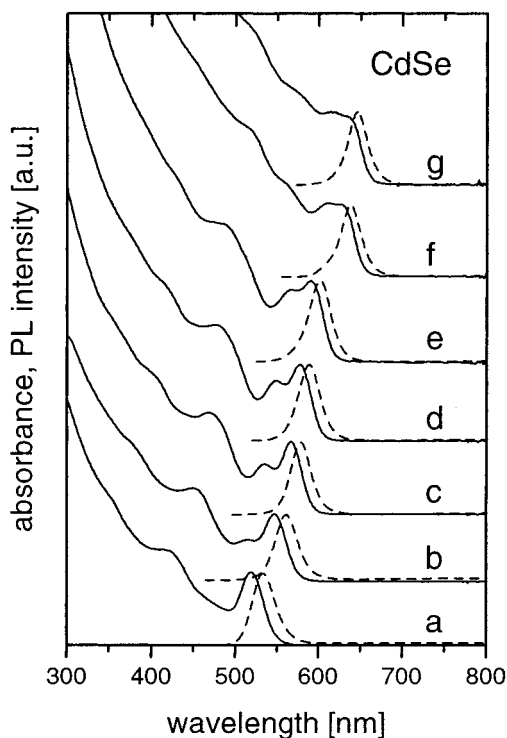


**Figure 1.** Room-temperature absorption and emission spectra of CdSe nanocrystals monitored during the growth at 300 °C.

CdSe nanocrystals were prepared by a modified high-temperature organometallic synthesis proposed by Murray et al.<sup>3</sup> All manipulations were performed using standard air-free techniques. The chemicals used were of analytical grade or of the highest purity available. HDA, TOPO, and TOP were additionally purified by distillation. In a typical synthesis, 1 mmol of TOPSe<sup>20</sup> and 1.35 mmol of dimethylcadmium were dissolved in 5 mL of TOP and rapidly injected into a vigorously stirred mixture of 10 g of TOPO (55 mol %) and 5 g of HDA (45 mol %) heated to 300 °C. Injection resulted in an immediate nucleation of nanoparticles displaying a broad adsorption maximum around 450 nm. Further growth occurred at 250–310 °C depending on the desirable size. The ratio between TOPO and HDA strongly affected the growth kinetics. The general tendency was that, with increasing HDA content, the initial particle size and the growth rate decreased. In mixtures containing more than about 80 mol % of HDA, precipitation of CdSe nanocrystals was observed above 200 °C. To prepare CdSe nanocrystals with sizes above 4.5–5.0 nm, additional injections of stock solution were required.

The growth dynamics of the nanocrystals was monitored by taking samples from the reaction mixture at different instants of time. All samples were immediately cooled and diluted with toluene to stop particle growth and to provide optical densities appropriate for PL measurements. All measurements shown in this paper were performed without any postpreparative size separation of nanocrystals. A set of absorption and photoluminescence spectra displaying the growth of CdSe nanocrystals at 300 °C is shown in Figure 1. The absorption spectra possess up to five resolved electronic transitions, indicating very narrow size distribu-

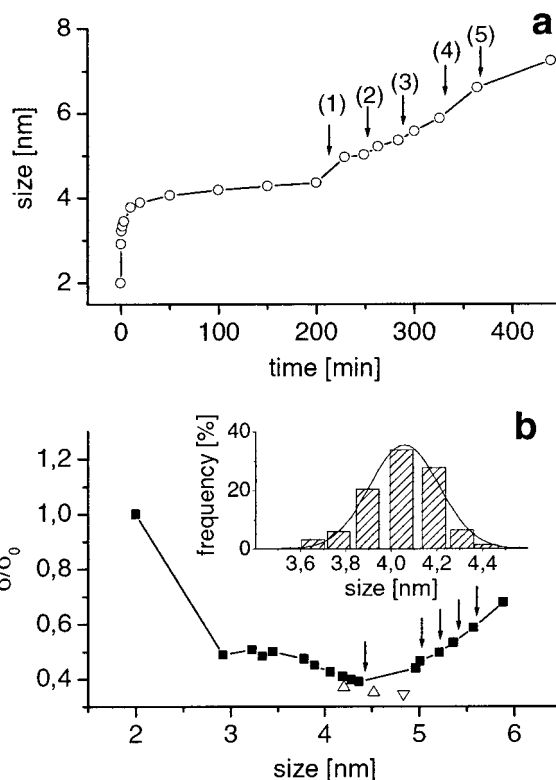


**Figure 2.** (a) Temporal dependence of the mean particle size during the growth of CdSe nanocrystals at 300 °C. (b) Relative particle size distribution of growing CdSe nanocrystals: (■) during continuous growth at 300 °C; (△) obtained after stepwise growth (1 h 250 °C + 1 h 280 °C) and (1 h 250 °C + 1 h 280 °C + 1 h 310 °C); (▽) obtained after slow additional injection of 0.4 mL of the stock solution at 280 °C to the stepwise grown nanocrystals. The inset shows a size histogram of CdSe nanocrystals with an average size of  $\sim 4.05 \pm 0.16$  nm measured from HRTEM images for over 200 particles. Arrows indicate additional injections of stock solutions containing (1)–(3) 50%, (4) 100%, and (5) 140% of Cd and Se precursors compared to the initial amount of CdSe.

tions of the CdSe nanocrystals, and are comparable with the best CdSe samples obtained by the TOPO–TOP synthesis followed by several stages of size-selective precipitation.<sup>3,6,21</sup>

Figure 2a shows the evolution of the mean particle size<sup>22</sup> during growth of the CdSe nanocrystals at 300 °C. The growth rate decreased gradually and the growth almost terminated when the particle size reached  $\sim 4.5$  nm. A rather low injection temperature (300 °C) and the use of purified solvents resulted in very reproducible growth kinetics of CdSe nanocrystals. The evolution of the particle size distribution during the growth at 300 °C was estimated from the absorption and PL spectra as reported previously<sup>21,22</sup> and shown in Figure 2b. As the size distributions estimated from optical spectra are systematically broader than the real ones,<sup>21</sup> we used relative values of standard deviation ( $\sigma$ ) normalized to a starting value ( $\sigma_0$ ) observed immediately after injection of the stock solution. A size histogram of the sample with average size of  $\sim 4.05 \pm 0.16$  nm measured from HRTEM images is shown as an inset to Figure 2b. In contrast to the growth of CdSe nanocrystals in TOPO–TOP,<sup>21</sup> very fast “focusing” of the size distribution was observed during the particle growth in HDA–TOPO–TOP and no “defocusing”

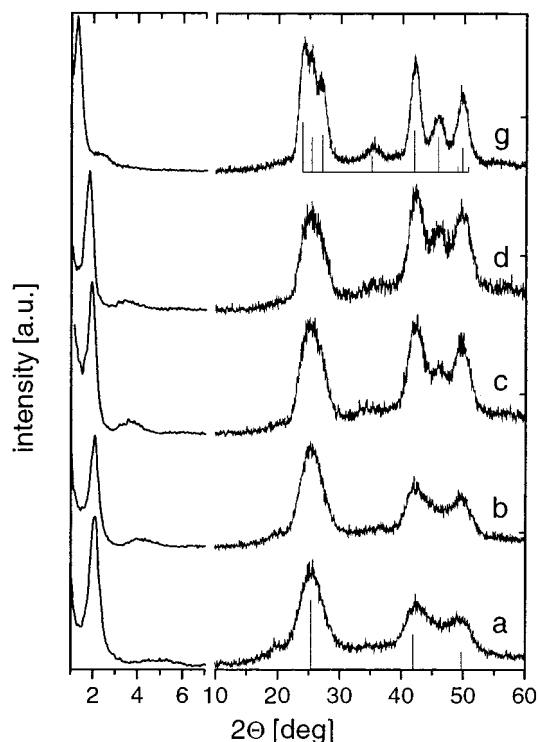


**Figure 3.** Small-angle and wide-angle powder X-ray diffractograms of a size series of CdSe nanocrystals (samples a–d and g from Figure 1). Vertical lines indicate bulk CdSe reflections (top: wurtzite, hexagonal; bottom: zinc blende, cubic).

after long-term heating at 300 °C. The observed permanent “focusing” of the size distribution might be a result of the large difference between the rate of nanocrystal growth in the “focusing” regime, which occurs due to the initial excess of the monomer in the solution,<sup>21</sup> and the rate of the Ostwald ripening process (“defocusing”). The growth of nanocrystals almost terminates after the “focusing” stage, and their size distribution remains narrow for a long time. The absence of “defocusing” means that the narrowest size distribution corresponds to the largest size achievable at a given growth temperature. As a result, stepwise growth (1 h at 250 °C + 1 h at 280 °C + 1 h at 310 °C) reproducibly allowed us to reach size distributions with a standard deviation below 4%. Additional injections of stock solution were required to obtain larger CdSe nanocrystals, which slightly broadened the size distribution (Figure 2b). This broadening is most probably caused by the high (300 °C) growth temperature resulting partly in new nucleation of nanocrystals. On the other hand, very slow (1 drop per 30 s) additional injection at 280 °C into a solution of CdSe nanocrystals primarily grown at 310 °C resulted in an even further narrowing of the size distribution. For all crude solutions of CdSe nanocrystals, the full widths at half-maximum (fwhm) of the band edge PL spectra were in the range of 27–31 nm.

Figure 3 shows small-angle and wide-angle P-XRD patterns of CdSe nanocrystals of different sizes. As expected, the width of the diffraction peaks at wide angles is considerably broadened and increases with decreasing particle size. Nanocrystals with sizes above ~4.0 nm exhibit P-XRD patterns with diffraction peaks in accord with those of

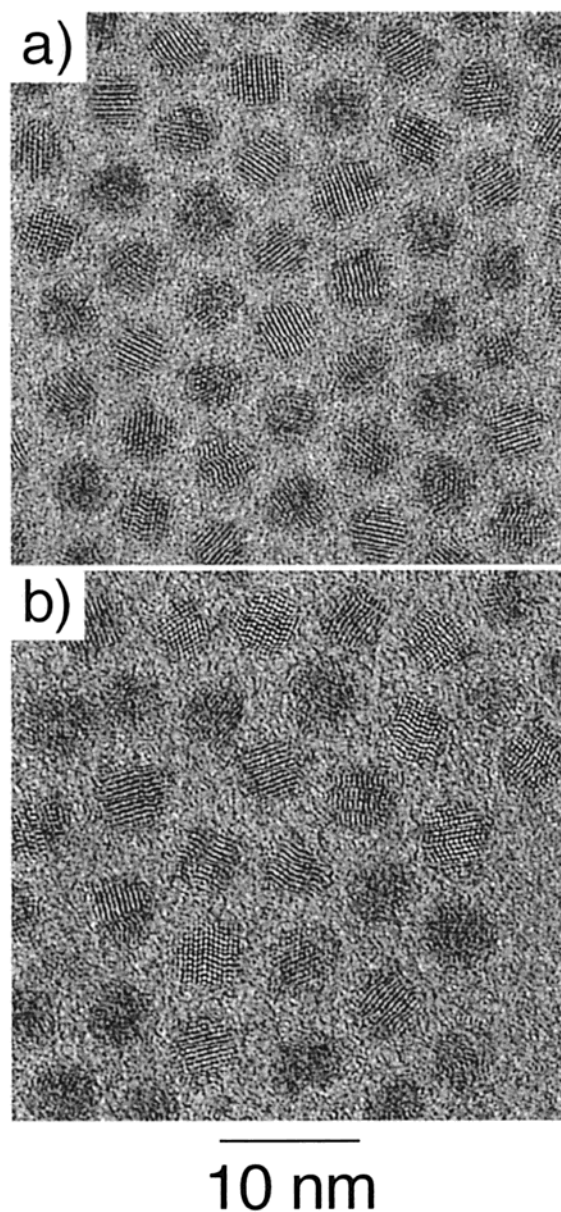


**Figure 4.** HRTEM images of (a) CdSe nanocrystals (sample c) and (b) CdSe/ZnS core–shell nanoparticles (CdSe sample c covered with 1.6 monolayers of ZnS).

hexagonal CdSe (wurtzite phase). In the case of smaller CdSe nanocrystals the XRD patterns do not permit to distinguish between the cubic and the hexagonal phases unambiguously. As it is often observed for nanocrystalline samples with narrow particle size distributions, the P-XRD patterns also show a very well pronounced sharp first-order reflex in the small-angle region (Figure 3), which is caused by Bragg diffraction on the nanocrystals ordered in the powder. The intensity of this reflex was ~3–5 times larger than that of the diffraction peaks at wide angles. Because of the exceptionally narrow size distribution of these CdSe nanocrystals, the second-order reflexes are also resolved (Figure 3).

HRTEM images of the CdSe nanocrystals (Figure 4a) show nearly spherical crystalline particles with lattice plane distances identical to hexagonal CdSe. EDX measurements



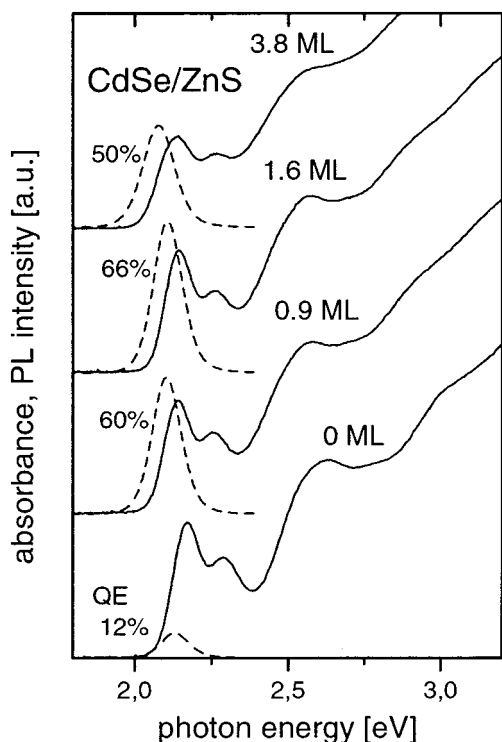


**Figure 5.** Room-temperature absorption and emission spectra of CdSe nanocrystals before and after deposition of ZnS shells of different thicknesses (in monolayers, ML).

indicate compositions close to the ratios given by the bulk formula. The narrow size distribution of the particle sizes resulted in a 2D hexagonal arrangement of CdSe nanocrystals on the TEM grids.

The room-temperature PL QE of as-prepared CdSe nanocrystals was in the range 10–25% and had a tendency to decrease with increasing particle size. However, the PL QE of the CdSe nanocrystals can be considerably improved by postpreparative surface passivation<sup>6,9,10,23</sup> with an inorganic (ZnS) or organic (amines) shell. This is a strong hint that the PL efficiency losses are due to insufficient passivation of the surface traps. Since CdSe quantum dots synthesized in the HDA–TOPO–TOP mixture showed an exceptionally narrow size distributions, no size selection and isolation of CdSe nanocrystals from the crude solution was required for the synthesis of core–shell particles. Moreover, a rather high initial concentration of CdSe cores can be used for the synthesis of core–shell particles.

In a typical synthesis of CdSe/ZnS core–shell nanocrystals, 2.5 mL of the crude solution of CdSe nanocrystals prepared as described above were mixed with 5 g of TOPO and 2.5 g of HDA and heated to 220 °C. The amount of Zn:S stock solution<sup>24</sup> necessary to obtain the desired shell thickness was calculated from the ratio between the core and shell volumes using bulk lattice parameters of CdSe and ZnS. This amount was then added dropwise to the vigorously stirred solution of CdSe nanocrystals. Figure 5 shows a set of absorption and PL spectra of CdSe/ZnS nanocrystals with different thicknesses of the shells. A maximum of the PL QE (66%) was observed for a ~1.6 monolayers thick ZnS shell and was reproducibly 50% or above for a wide range

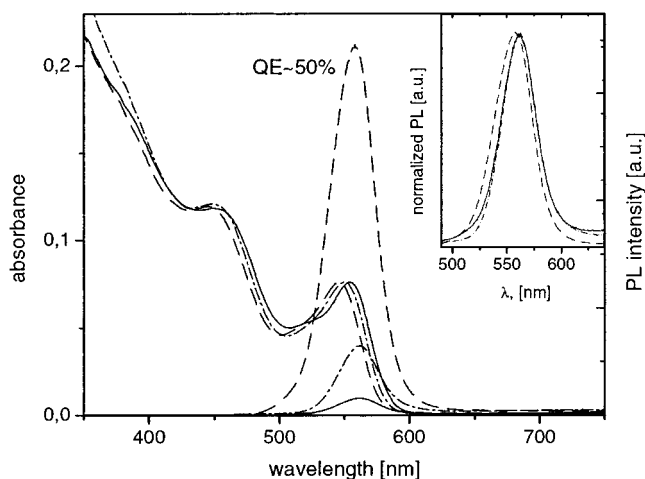


**Figure 6.** Room-temperature absorption and emission spectra of TOPO-capped 3.7 nm CdSe nanocrystals before (solid lines) and after (dashed lines) surface exchange with allylamine. The spectra taken after partial reconstruction of the initial TOPO–TOP stabilizing shell are presented as dash–dot lines. The inset shows normalized PL spectra.

of the shell thicknesses and core sizes. Figure 4b shows a HRTEM image of CdSe/ZnS nanocrystals (1.6 monolayers of ZnS) synthesized from ~4.0 nm large CdSe cores shown in the Figure 4a.

It was also found that the postpreparative treatment of CdSe nanocrystals with primary amines, e.g., allylamine or dodecylamine (DDA) resulted in a significant improvement of the PL QE as well. The passivation of the CdSe surface with amines was performed according to the following recipe: 1 mL of the crude solution of CdSe nanocrystals was mixed with 5 mL of allylamine or DDA and subsequently stirred at 50 °C (allylamine) or 100 °C (DDA) for 24 h. The nanocrystals were precipitated with methanol and redispersed in hexane for optical measurements. All manipulations were carried out inside the glovebox to prevent oxidation of the nanocrystals. The surface exchange led to a stable PL with QE of 40–50% in both cases, which is comparable to values for CdSe nanocrystals covered with inorganic shells. This enhancement of the band edge PL in comparison with TOPO-capped CdSe nanocrystals may be the result of a strong bonding of the amines to the nanocrystal surface, which allows its better passivation. Less sterically hindered amines may improve surface capping and, hence, the passivation of traps by creating larger capping densities.<sup>8,13</sup>

The influence of amines on the PL properties of CdSe nanocrystals has been further investigated by the substitution of TOPO at the surface of CdSe nanocrystals synthesized via conventional TOPO–TOP synthesis. After treatment of the nanocrystals with allylamine or DDA the band edge PL increased by about an order of magnitude (Figure 6) and reached a QE of ~50%. Exchange of TOPO by amines at the surface of CdSe nanocrystals was accompanied by a slight blue shift of both the absorption spectrum edge and the maximum of the band edge PL band (Figure 6). Allylamine can be partially removed from the particle surface

by precipitating the nanocrystals from the amine–TOPO–TOP solution, redissolving them in TOPO–TOP mixture, and subsequently pumping off allylamine in a vacuum at 60 °C. This partial reconstruction of the initial TOPO/TOP stabilizing shell was accompanied by a red shift of both the absorption and the PL spectra (Figure 6). The blue shift during the exchange of TOPO with amine might be explained either by a slight decrease of the particle size caused by losing surface Cd and Se atoms with leaving TOPO molecules<sup>3,7</sup> or by a redistribution of electronic density in the semiconductor core under the influence of passivating groups. The reversibility of the spectral shift during the amine-to-TOPO exchange allows us to suppose the latter explanation as responsible for the behavior observed.

In summary, exceptionally monodisperse CdSe nanocrystals were synthesized by introducing alkylamines into the widely used TOPO–TOP synthesis. The use of purified stabilizing agents resulted in highly reproducible growth dynamics, shape, and PL QE of CdSe nanocrystals. Continuous focusing of the size distribution occurred during the entire growth process, which makes the need of postpreparative size selective fractionation unnecessary. CdSe nanocrystals synthesized in HDA–TOPO–TOP can be successfully used as prepared for the synthesis of core–shell CdSe/ZnS nanoparticles with high reaction yields and PL QE of 50–60%. Alkylamines effectively passivated the surface of CdSe nanocrystals allowing to reproducibly reach PL QE of 40–50% at room temperature. These features may significantly broaden the possibility of using CdSe nanocrystals for display and tagging applications.

**Acknowledgment.** We thank Johanna Kolny for assistance with P-XRD measurements. This work was supported by the research project of the University of Hamburg and Philips. A.L.R. is indebted to the Alexander von Humboldt Foundation for providing a research scholarship.

## References

- (1) Efros, A. L.; Efros, A. L. *Sov. Phys. Semicond.* **1982**, *16*, 772.
- (2) Rossetti, R.; Nakahara, S.; Brus, L. E. *J. Chem. Phys.* **1983**, *79*, 1086.
- (3) Murray, C. B.; Norris, D. J.; Bawendi, M. G. *J. Am. Chem. Soc.* **1993**, *115*, 8706.
- (4) Bowen Katari, J. E.; Colvin, V. L.; Alivisatos, A. P. *J. Phys. Chem.* **1994**, *98*, 4109.
- (5) Eychemüller, A. *J. Phys. Chem. B* **2000**, *104*, 6514.
- (6) Dabbousi, B. O.; Rodriguez-Viejo, J.; Mikulec, F. V.; Heine, J. R.; Mattoussi, H.; Ober, R.; Jensen, K. F.; Bawendi, M. *J. Phys. Chem. B* **1997**, *101*, 9463.
- (7) Kuno, M.; Lee, J. K.; Dabbousi, B. O.; Mikulec, F. V.; Bawendi, M. G. *J. Chem. Phys.* **1997**, *106*, 9869.
- (8) Peng, X.; Schlamp, M. C.; Kadavanich, A.; Alivisatos, A. P. *J. Am. Chem. Soc.* **1997**, *119*, 7019.
- (9) Hines, M. A.; Guyot-Sionnest, P. *J. Phys. Chem.* **1996**, *100*, 468.
- (10) Peng, X.; Manna, L.; Yang, W. D.; Wickham, J.; Scher, E.; Kadavanich, A.; Alivisatos, A. P. *Nature* **2000**, *404*, 59.
- (11) Manna, L.; Scher, E. C.; Alivisatos, A. P. *J. Am. Chem. Soc.* **2000**, *122*, 12700.
- (12) Peng, Z. A.; Peng, X. *J. Am. Chem. Soc.* **2001**, *123*, 183.
- (13) Hines, M. A.; Guyot-Sionnest, P. *J. Phys. Chem. B* **1998**, *102*, 3655.
- (14) Norris, D. J.; Yao, N.; Charnock, F. T.; Kennedy, T. A. *Nano Lett.* **2001**, *1*, 3.
- (15) Schlamp, M. C.; Peng, X.; Alivisatos, A. P. *J. Appl. Phys.* **1997**, *82*, 5837.
- (16) Mattoussi, H.; Radzilowski, L. H.; Dabbousi, B. O.; Thomas, E. L.; Bawendi, M. G.; Rubner, M. F. *J. Appl. Phys.* **1998**, *83*, 7965.
- (17) Gao, M.; Lesser, C.; Kirstein, S.; Möhwald, H.; Rogach, A. L.; Weller, H. *J. Appl. Phys.* **2000**, *87*, 2297.
- (18) Bruchez, M. P.; Moronne, M.; Gin, P.; Weiss, S.; Alivisatos, A. P. *Science* **1998**, *281*, 2013.
- (19) Chan, W. C. W.; Nie, S. *Science* **1998**, *281*, 2016.
- (20) Preparation of TOPSe is described in refs 3 and 4.
- (21) Peng, X.; Wickham, J.; Alivisatos, A. P. *J. Am. Chem. Soc.* **1998**, *120*, 5343.
- (22) Sizes and size distributions were estimated from the absorption and PL spectra as described in ref 17 using sizing curves for CdSe quantum dots from the Supporting Information of ref 17 and to the paper by F. V. Mikulec, M. Kuno, M. Bennati, D. A. Hall, R. G. Griffin, M. G. Bawendi: *J. Am. Chem. Soc.* **2000**, *122*, 2532.
- (23) Gao, M.; Kirstein, S.; Möhwald, H.; Rogach, A. L.; Kornowski, A.; Eychemüller, A.; Weller, H. *J. Phys. Chem. B* **1998**, *102*, 8360.
- (24) Composition of the Zn:S stock solution: 0.4 mmol of diethylzinc and 0.51 mmol of bis(trimethylsilyl) sulfide in 3 mL of TOP.

NL0155126